Int. J. Electrochem. Sci., 8 **(2013)** 8966 - 8977

International Journal of
ELECTROCHEMICAL
SCIENCE
www.electrochemsci.org

Electrocapacitive Properties of $MnFe_2O_4$ Electrodes in Aqueous $LiNO_3$ Electrolyte with Surfactants

Baoyan Wang[1,2], *Peizhi Guo*[1,2,*], *Huaqing Bi*[1,2], *Qun Li*[1,2], *Guoliang Zhang*[1,2], *Rongyue Wang*[1,2], *Jingquan Liu*[1,2], *and X. S. Zhao*[1,2,3]

[1] Laboratory of New Fiber Materials and Modern Textile, the Growing Base for State Key Laboratory, Qingdao University, Qingdao, P. R. China. Fax: +86 532 8595 5529; Tel: +86 532 8595 1290;
[2] School of Chemistry, Chemical Engineering and Environment, Qingdao University, Qingdao, P. R. China.
[3] School of Chemical Engineering, The University of Queensland, St Lucia, QLD 4072, Australia
[*]E-mail: pzguo@qdu.edu.cn; guopz77@yahoo.com

Received: 5 May 2013 / *Accepted:* 7 June 2013 / *Published:* 1 July 2013

The electrocapacitive properties of $MnFe_2O_4$ hollow spheres and colloidal nanocrystal clusters in electrolyte $LiNO_3$ containing surfactants were studied. Electrochemical performances of supercapacitors were evaluated by cyclic voltammetry (CV), galvanostatic charge–discharge, self-discharge, cycle stability and electrochemical impedance spectroscopy (EIS). Results showed that the $MnFe_2O_4$ colloidal nanocrystal clusters electrode displayed a higher capacitance than that of $MnFe_2O_4$ hollow sphere. Anionic surfactant sodium dodecyl sulphate (SDS) and non-ionic surfactant p-t-octylophenol (Triton-X-100) and poly(ethylene glycol)-block-poly(propylene glycol)-block-Poly(ethylene glycol) (P123) were added respectively to $LiNO_3$ electrolyte to investigate capacitive features of $MnFe_2O_4$-nanocrystal-based supercapacitors. It was found that lowering the interfacial tension between the electrode and electrolyte favoured the diffusion of lithium ions. For example, surfactant SDS enhanced 36.8% capacitance with an energy density of 14.5 Wh/Kg at the current density of 0.05 A/g, and the capacitive retention was 82% after 1000 cycles. However, the capacitance improves about 22.8% and 12.8% after the addition of Triton-X-100 and P123, respectively. Based on the experimental results, the enhancement mechanism of surfactants on the electrochemical performances of the as-prepared supercapacitors was proposed.

Keywords: Manganese ferrite; Colloidal nanocrystal cluster; Supercapacitor; Surfactant

1. INTRODUCTION

Supercapacitors, also named as electrochemical capacitors, have attracted a lot of attention in energy storage devices due to their important applications, such as hybrid electric vehicles, mobile electronic devices and memory backup systems [1-3], because they can simultaneously provide high

power density and energy density. Generally speaking, supercapacitors can be divided into two categories by the energy storage mechanism: electrical double layer capacitors (EDLCs) and pseudocapacitors. The EDLCs utilize the electrostatic separation of charges at the electrode/electrolyte interface to improve the capacitance, which depends on the specific surface area of materials [4]. However, pseudocapacitors store energy by charge transfer through surface Faradaic redox reactions between electrode and electrolyte.

The energy density and power density of pseudocapacitors are usually several times larger than those of EDLCs [5]. The first discovered electrode material for pseudocapacitor is RuO_2 [6]. It was demonstrated that its specific capacitance reached 700 F/g [7], wheras, the high cost limited its wide application. In order to prepare affordable electrode, other materials such as cobalt oxide [8], nickel oxide [9] and manganese oxide [10] were investigated. For more practical applications, supercapacitors with higher operating voltage and higher energy density without sacrificing cycle life [11] are desired. However, in aqueous electrolyte, the operating voltage, which plays an important role in improving the energy density, according to the equation: $E=1/2\ CV^2$, is restricted by water decomposition voltage. Therefore, developing novel supercapacitors with high performances and operating voltages in aqueous electrolyte is still in great demand [12,13].

To achieve capacitance enhancement, it is also possible to modify the electrode material by applying conducting polymer [14,15] or assembly with asymmetric system [16,17]. However, the complicated process and/or the high cost limit the industrial application. Therefore, other strategies including adding surfactants into the electrolyte are explored [18]. Surfactants can be immobilized on the electrode surface via varied interactions, such as electrostatic interactions, coulomb interactions, hydrogen bonding, or noncovalent bonding between their hydrophobic (water-hating) or hydrophilic (water-liking) groups and the surface bound inorganic precursors [19,20] Addition of surfactants in supercapacitors can lower the surface tension, therefore it may be an effective means to enhance the electrochemical properties [21]. In addition, the surfactants cannot deteriorate the electrochemical properties of the cells at high temperature, thus their cycle-life and storage performance maximally protected [22]. Therefore, various surfactants were explored to reduce the surface intention for improved capacitance. For example, anionic surfactant had been utilized to improve discharge capacitance and surface passivation of zinc anode [23]. Recently, ferrite was used as electrode materials to fabricate electrochemical capacitors under neutral or alkali electrolytes [5,24]. However, the effect of surfactants in aqueous electrolytes as well as the microstructure of ferrite nanomaterials on the performances of pseudocapacitors still remains a burning question.

In this work, we discussed the capacitive performances of $MnFe_2O_4$ hollow sphere-based supercapacitor (SC-HS) and colloidal nanocrystal cluster (CNC)-based supercapacitor (SC-CNC) in aqueous $LiNO_3$ electrolyte. The operating voltage can be enlarged in a wide range in aqueous electrolyte compared with the decomposition voltage of water and thus the energy density can be improved significantly. The capacitive performances of CNC-based supercapacitors were further investigated based on $LiNO_3$ electrolyte containing various surfactants including SDS, Triton-X-100 and P123 and the corresponding supercapacitors are named as SC-SDS, SC-TX-100 and SC-P123, respectively. Meanwhile, the mechanism about how the surfactants induce the surface intention was also proposed. In addition, electrochemical performances of $MnFe_2O_4$-based supercapacitors were

evaluated by cyclic voltammetry (CV), galvanostatic charge–discharge, self-discharge, cycle stability and electrochemical impedance spectroscopy (EIS). Upon the addition of SDS, the capacitance of SC-SDS was improved 36.8% compared to that of pure $LiNO_3$ electrolyte (SC-CNC) at 0.05 A/g, the capacitive retention still retained 82% after 1000 cycles, and the energy density can reach 14.5 Wh/Kg at 0.05 A/g.

2. EXPERIMENTAL

2.1Materials and preparation

All chemicals, including $Mn(CH_3COO)_2 \cdot 4H_2O$, $FeCl_3 \cdot 6H_2O$, CH_3COONa, SDS, cetyltrimethyl ammonium bromide (CTAB), ethylene glycol, and $LiNO_3$ were of analytical grade (Sinopharm Chemical Reagent Company). Triton-X-100 and P123 were purchased from Aldrich. Acetylene carbon black (99.99%) and polytetrafluoroethylene latex (PTFE 60 wt. %) were purchased from Strem Chemicals and Aldrich, respectively. The preparation of $MnFe_2O_4$ was carried out following the procedure as descirbed in the literature [25]. As additive, concentration of surfactant was 5 mM unless otherwise specified. Double distilled water was used in the experiments.

2.2 Characterization

Transmission electron microscopy (TEM) images were obtained with a JEM-2000EX transmission electron microscope operated at 160 kV [25].

2.3 Electrochemical measurements

The electrodes were prepared from well-mixed slurry containing 80wt. % active materials, 5 wt. % PTFE, and 15 wt. % acetylene carbon black. The slurry was pressed onto a nickel foam substrate (1 cm^2) at 1.5 MPa, followed by drying in a vacuum oven at 120^oC for 12 h. The typical mass load of the active material in an electrode was about 6 mg. Cyclic voltammetry, galvanostatic charge/discharge curves and electrochemical impedance spectra were collected using a two-electrode cell. The two-electrode cell was composed of two collectors, two electrodes and a porous fibrous separator based on aqueous 2 M $LiNO_3$ electrolyte without or with various surfactants. All electrochemical tests were measured in a CHI760D electrochemical workstation (CH Instrument, USA). All measurements were carried out at room temperature.

3. RESULTS AND DISCUSSION

To explain the electrochemical results, it is important to consider the size and shape of ferrite materials which play important roles in charge storage. Recently, we demonstrated that hollow sphere and well-seperated CNC of $MnFe_2O_4$ with submicron scales [25] can be synthesized in a controlled

manner using solvothermal method as shown in Figure 1. It had been reported that ferromagnetic hollow spheres were composed of $MnFe_2O_4$ nanocrystals with the size of about 20 nm while superparamagnetic CNC were formed by the assembly of small nanocrystals of about 5 nm in highly-prefered orientation [25]. From the point of practical applications, $MnFe_2O_4$ CNC-based electrochemical devices has also been superior to those based on dispersed $MnFe_2O_4$ nanoparticles because CNC should show higher density than dispersed nanocrystals due to its unique structure.

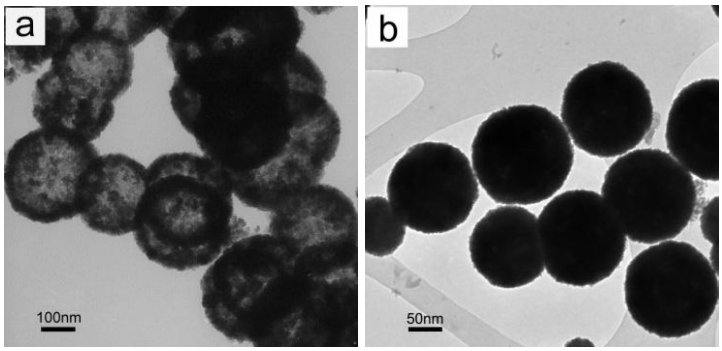

Figure 1. TEM images of $MnFe_2O_4$ hollow spheres (a) and CNCs (b).

Cyclic voltammograms (CVs) of $MnFe_2O_4$-based two-electrode supercapacitors, taking SC-CNC as an example, were conducted consecutively in a large voltage range as shown in Figure 2. Supercapacitors with aqueous electrolyte are supposed to be operated in voltage windows lower than 1.23 V, namely the theoretical decomposition voltage of water. The operating voltage higher than this will lead to the evolution of oxygen and hydrogen due to the water electrolysis. In fact, for the application of energy storage in aqueous supercapacitors, especially in pseudocapacitors, the operating voltage can be enlarged due to the existence of overpotential under the gas evolution. It can be seen from Figure 2 that the typical capacitive behavior can be observed in a potential range of -0.4~1.5 V, showing an almost rectangular profile. Further enlarging the voltage to 1.6 V would generate non-ideal electrochemical reactions as can be observed in Figure 2.

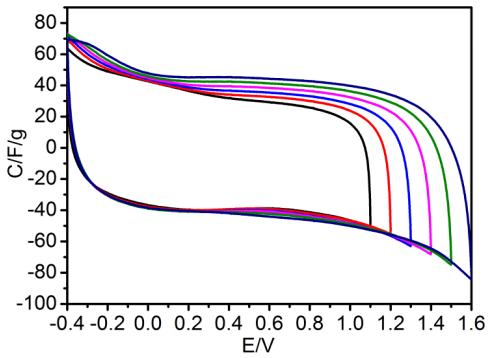

Figure 2. CV curves of SC-CNC under different voltage windows. Scan rate: 20 mV/s.

This paper aims to study two aspects of $MnFe_2O_4$-based supercapacitors: (1) the effect of the structure of $MnFe_2O_4$ samples on their capacitive features, (2) the effect of surfactants in aqueous electrolyte on their electrochemical performances. Thereafter, the voltage window in the following studies was set in the potential range of -0.4~1.2 V.

Figure 3A shows the CV curves of aqueous SC-HS and CNC-based supercapacitors (CNC-SCs) without and with the addition of surfactants at the scan rate of 20 mV/s. Clearly, the CV curves of all the CNC-SCs shows a more rectangular shape than that of hollow spheres in a potential range of -0.4~1.2 V. Furthermore, the area of the CV curve of SC-HS is much smaller than that of SC-CNC, indicating that the capacitance of SC-HS is much lower than that of SC-CNC. This should be ascribed to the differences in the structure and crystalline size between the hollow spheres and CNCs (Figure1). On the one hand, small nanocrystals aggregate orderly and develop colloidal clusters, which means that CNCs would exhibit higher surface area and larger effective contact between the active materials and the electrolyte [26]. On the other hand, agglomeration, which can be demonstrated through TEM, exists among hollow spheres, would result in the decrease of effectively available channel for electrolytic ions [23]. That leads to the compromised transport of electrolytic ions. So, we focused on the effect of surfactants on the electrochemical properties of four types of CNC-SCs in the following studies.

Wu and Kuo evidenced the presence of a redox hump of the ferrite electrodes in aqueous NaCl electrolyte [5]. However, in current research no obvious hump of CVs was found in $LiNO_3$ electrolyte as shown in Figure 3A. In addition, a rectangular profile presenting capacitive performance was found in the organic lithium ion electrolyte [27]. These indicate that the mechanism of $MnFe_2O_4$ in aqueous lithium ion solutions is similar to that of lithium ion battery. There is valence change at Mn-ion sites, which is close to the pseudocapacitive mechanism of MnO_2, in response to Li-ion insertion/extraction. Furthermore, as an aqueous capacitor, the potential window was improved to a larger voltage range than the theoretical decomposition voltage of water, which provides a favourable factor on improving the energy storage of the supercapacitors.

As depicted in Figure 3, the CV curves of CNC-based supercapacitors containing surfactants show similar rectangular profiles with that of SC-CNC, suggesting the existence of good pseudocapacitive behaviour. Interestingly, three obvious features can be derived from the CVs of supercapacitors with and without surfactants. Firstly, owing to the addition of surfactants, the capacitance of supercapacitors improves significantly compared to that of SC-CNC. This is probably because that decreasing the interfacial tension between electrode and electrolyte has a positive effect on the permeation of lithium ions [20]. Secondly, the nature of surfactants shows distinct effect on the capacitance and the capacitance for the four types of CNC-SCs obeys the order of SC-SDS>SC-TX-100>SC-P123>SC-CNC. Thirdly, compared with the profile at the scan rate of 20 mV/s, the shape of the CV curve is almost unchanged at 100 mV/s when adding SDS. However, the rectangular profile shows a slight distortion in SC-TX-100 and SC-P123 at 100 mV/s. In addition, the rectangular profile displays a serious distortion in SC-CNC. These show that even if at a high scan rate, the $MnFe_2O_4$ electrode can still exhibit good pseudocapacitive behavior because of the addition of surfactant,

Above all, adding SDS into the electrolyte of the supercapacitors has a positive effect on the capacitance and the retention of rectangular shape of CVs at different scan rates. The effect of the SDS

concentrations on the electrochemical properties of CNC-based supercapacitors has also been investigated. As shown in Figure S1 when the concentration of SDS is below critical micelle concentration (CMC=8.7×10^{-3} M), the capacitance increases with the increasing concentration of SDS. When the SDS concentration reached 10 mM, the capacitance decreased compared with that of 5 mM. These may be attributed to the formation of micelles, which reduces the effective utilization of SDS. These are in accordance with the proposed mechanism on the effect of surfactants (scheme 1).

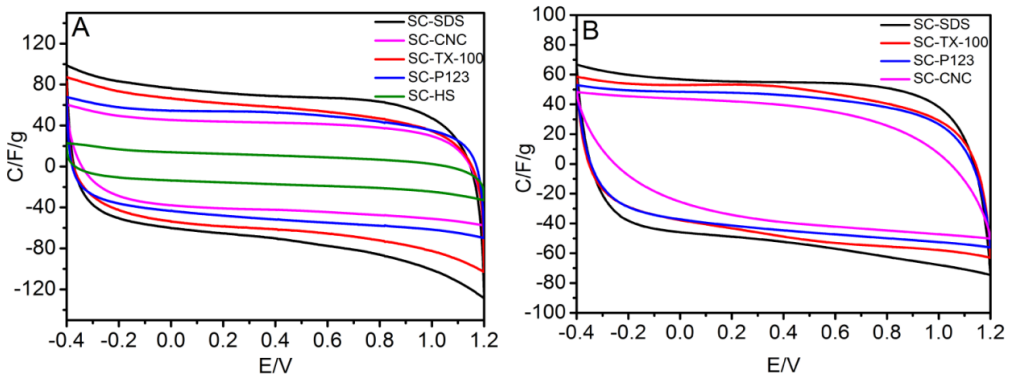

Figure 3. CV curves of SC-HS and CNC-SCs at the scan rates of 20 mV/s (A) and 100 mV/s (B).

Figure 4A shows galvanostatic charge/discharge curves of $MnFe_2O_4$-based supercapacitors at the current density of 0.05 A/g. The symmetric shape of galvanostatic curves indicates that there is no accompanying redox phenomenon during the process and the surfactants remain stable in the applied potential window [18]. Furthermore, the time accomplishing one charge/discharge cycle for SC-HS is much shorter than that of any of CNC-based cells, indicating the smallest capacitance for hollow sphere. The capacitances for all the four types of CNC-SCs are following the order of SC-SDS>SC-TX-100>SC-P123>SC-CNC, which is in accordance with those results of CVs, further confirming the existence of the positive effect on the electrochemical performances due to the addition of surfactants into the aqueous electrolyte.

Owing to the introduction of SDS, the capacitance increased from 53.3 F/g of SC-CNC to 73.7 F/g of SC-SDS at 0.05 A/g, namely 36.8% improvement achieved, as calculated from Figure 4A. The capacitance improved about 22.8% and 12.8% upon the addition of Triton-X-100 and P123 into the electrolyte, respectively. Figure 4B shows the capacitance variations as a function of the current density of CNC-SCs. It can be seen that the capacitive retention of the SC-SDS is about 74.5% in the current density range from 0.05 A/g to 2 A/g, 62.1% for SC-TX-100, 72.2% for SC-P123 and 46.5% for SC-CNC. These results evidenced that adding surfactants into the electrolyte gives better capacitive retention than SC-CNC, and the addition of SDS exhibited the best performance.

A good linear relation of IR drop during charge/discharge processes as a function of time indicated small equivalent resistance and ideal capacitive characteristic (Figure 4C). However, the inner resistance values can also be determined from the slope. As shown in Figure 4C SC-SDS has minor inner resistance (IR = 0.00835+0.0805 I), which favours the high discharge energy device in

practical application.16 The order of inner resistance of supercapacitors is SC-CNC>SC-P123>SC-TX-100>SC-SDS as derived from the slope of lines in Figure 4C.

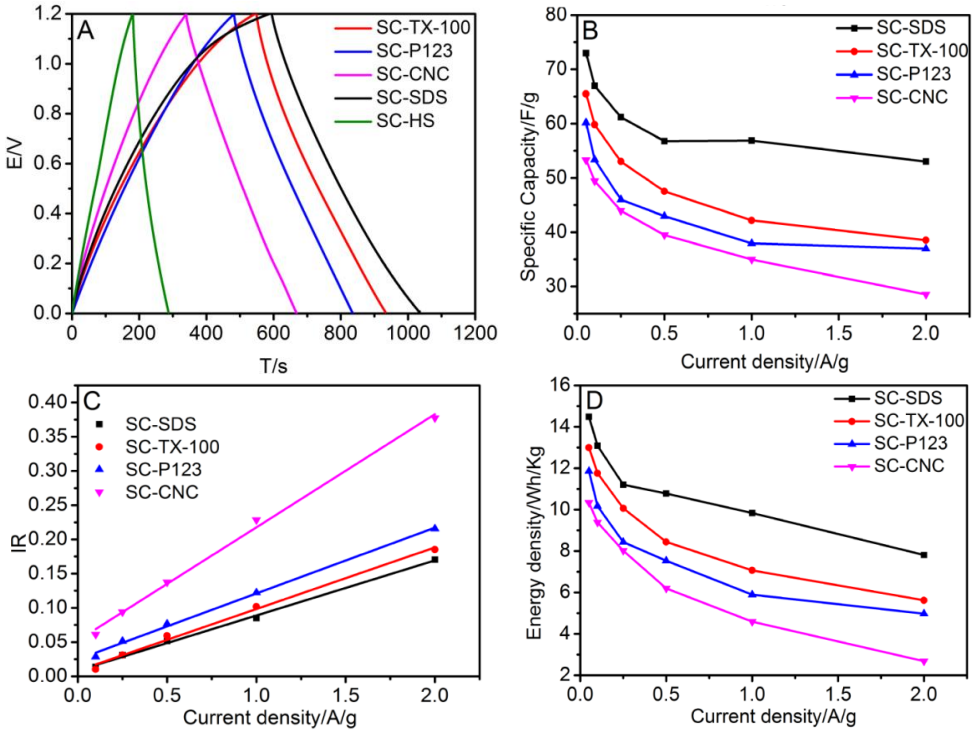

Figure 4. (A) Galvanostatic charge–discharge curves of SC-HS and CNC-SCs at the current density of 0.05 A/g. (B) Capacitive curves of CNC-SCs at different current densities. (C) IR variation as a function of the current density in CNC-SCs. (D) Energy density as a function of the current density in CNC-SCs .

According to $E = 1/2\ C\Delta V^2$, where C is capacitance and ΔV is the working voltage window, E is proportional to C when the value of ΔV keeps constant. Therefore, the supercapacitors with the addition of surfactants possess higher energy density than SC-CNC, where SC-SDS exhibited the highest energy density among CNC-SCs. It can be seen from Figure 4D that the energy density of SC-SDS is 14.5 Wh/Kg at the current density of 0.05 A/g, which is about 1.4 times that of SC-CNC. Clearly, the SC-SDS also displayed the highest energy density retention values among CNC-SCs. Furthermore, the higher the current density, the larger energy density percentage SC-SDS has. In addition, the order of energy density was found to be similar to that of capacitance among various electrolytes.

According to the analytical results of Figure 3 and 4, the effect of surfactant on the electrochemical performance of supercapacitor is closely related to the nature of the surfactant. The mechanism for the improvement of electrochemical performances of supercapacitors by various surfactants is proposed. (Scheme.1) The decreased surface tension should be expected upon the addition of surfactant. The factors of determining surface effective value are versatile. The chain length of hydrophobic group, the existence of branched-chain and unsaturated degree of bond are expected to

be the decisive factors in the present study. When unsaturated degree of hydrophobic group and branched-chain are improved, and the chain length of hydrophobic group becomes smaller, the surfactant effective value can be significantly increased. As shown in scheme 1, the chain length of hydrophobic group in SDS is the smallest among the three surfactants, displaying the highest effective value. Comparing with P123, Triton-X-100 has the higher branched-chain and unsaturated bonding degree owing to the existence of benzene, thus it should have higher surfactant effective value. On the other hand, critical micelle concentration of Triton-X-100 is 2.5×10^{-4} M [28], therefore, micelle should be formed at electrolyte concentration of 5 mM. Meanwhile, in dilute aqueous solutions, the PEO-PPO-PEO may form micelles [29] while SDS cannot. The selected concentration of SDS is also crucial for the enhancement of electrochemical performances of SC-SDS. If the SDS concentration is lower than 5 mM or higher than CMC, the electrochemical performances of such supercapacitors are lower than that of SC-SDS, as shown in Electronic Supplementary Information (ESI) Figure 1. It should also be pointed out that the supercapacitors with CTAB showed similar electrochemical performances with the supercapacitors with SDS.

The electrochemical impedance spectroscopy (EIS) was performed to probe the electrochemical characteristics of the electrode/electrolyte interface of supercapacitors. It is shown in Figure 5 that in all cases, the EIS spectra exhibit a high frequency semicircle and a low frequency sloping line. The low frequency sloping line is controlled by the diffusion of Li^+ through electrolyte, which means a capacitive behavior [30]. Furthermore, the low frequency sloping lines become steep obviously with the addition of surfactants, indicating the enhancement of capacitance, a result which is similar to those of CVs and galvanostatic charge–discharge measurements. The high frequency semicircle observed in this work is related to the interfacial electron transfer resistance [31]. Generally, addition of surfactants would decrease the surface tension, therefore, the interfacial electron transfer resistance becomes smaller than that of SC-CNC. Micelles were formed in the electrolytes containing P123 and Triton-X-100 (Scheme 1), therefore, the ionic surface of micelles should also result in accelerating the rate of interfacial electron transfer.

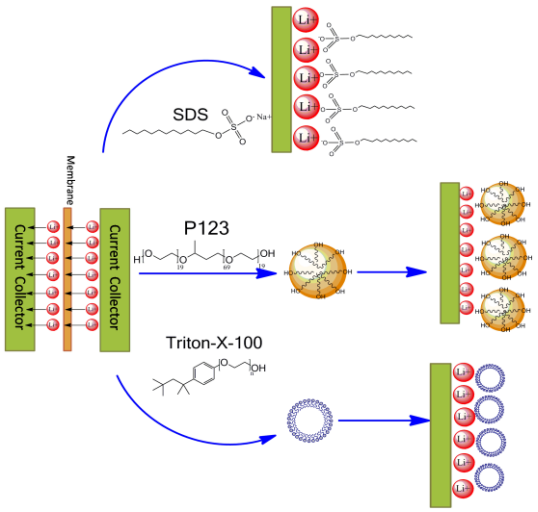

Scheme 1. The enhancement mechanism of surfactants on the electrochemical performances of $MnFe_2O_4$-based supercapacitors.

In the equivalent circuit, the solution resistance (Rs) refers to the resistance from the electrolyte [32], and the charge-transfer resistance (Rct) corresponds to the total resistance at the interface between the electrode and the electrolyte. The parallel Rct and $C_{D.L.}$ configurations account for the semicircle feature, while arising from the pseudocapacitance of $MnFe_2O_4$, C_P accounts for the steep line. Rs, known as the equivalent series resistance (ESR), corresponds to the resistance of the bulk electrolyte solution, which is estimated from the real axis intercept at high frequency [33,34]. As shown in Figure 5, the magnitude of ESR of SC-SDS is lower than that of SC-TX-100 or SC-P123, which is caused by the small SDS molecule existing in electrolyte. In addition, the magnitude of ESR of SC-P123 is obviously larger than that of SC-TX-100, which indicated that P123 formed larger micelle than Triton-X-100 in the electrolytes (Scheme 1). However, the existence of micelles with a large size would impede the transport of ions.

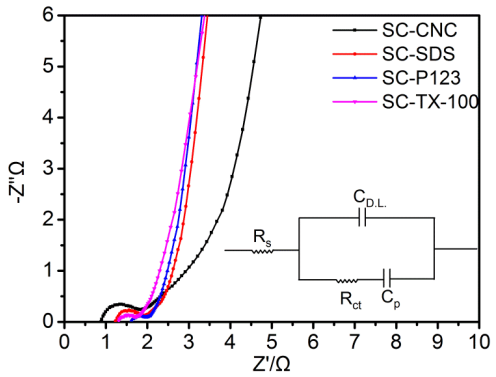

Figure 5. Nyquist plots of four types of CNC-SCs in the ranges of frequency from 0.01 HZ-100 KHZ under open circuit potential conditions. The inset is the equivalent circuit of Nyquist plots.

Taking into account that supercapacitor plays an important role in electronic devices and self-discharge is an inevitable undesired phenomenon.

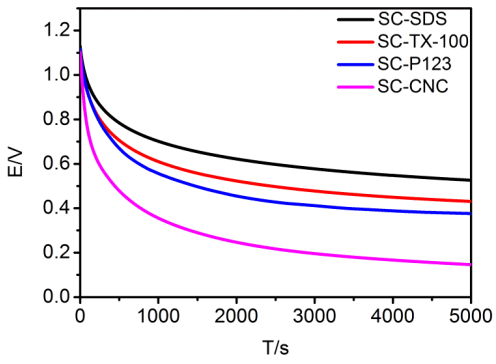

Figure 6. Self-discharge curves of four types of CNC-SCs.

The self-discharge performances of supercapacitors with various surfactants were also investigated by charging the cells up to 1.2 V and then opening the circuit while recording the

variation of the cell voltage with time [35]. As shown in Figure 6 the self-discharge capacity is far less than charge/discharge capacity, however, slowly decrease of the capacity still observed. The self-discharge curves evidenced that the presence of surfactants decreased the self-discharge value. Moreover, SC-SDS exhibited a much slower self-discharge rate than SC-TX-100 and SC-P123, which is in accordance with those derived from Figure 3-5. Good cycle ability is one of the most important demands for supercapacitors. Figure 7 shows the capacitance against the cycle number of four types of CNC-SCs. After 1000 cycles, the capacitance decreases slowly for pseudocapacitance in the pure $LiNO_3$ electrolyte [36]. All symmetric supercapacitors with added surfactants are found to exhibit a better cycle life than in pure $LiNO_3$ electrolyte over the entire cycle-number range, which means that cycle ability can be improved significantly by the addition of surfactants in the electrolyte. After 1000 cycles, the SC-SDS retains 82% of its initial specific capacitance, which indicates that the electrode material has a high degree of reversibility [37]. Comparing with Triton-X-100 and P123, SDS is one type of small molecule and becomes ionization during charge/discharge process. In addition, the formation of large-scale micelles for Triton-X-100 and P123 (Scheme 1) may block the channel and the surface of electrode during long time charge/discharge measurements and thus lead to a lower cycle ability. However, the moderate concentration of SDS in SC-SDS provides the proper spacial configuration and fast charge transfer features, both of which would improve the performances of CNC-based cells. These results should give the valuable clues for optimization of supercapacitor fabrications.

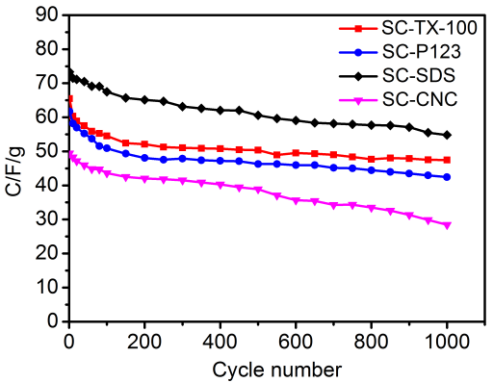

Figure 7. Cycle stability of four types of CNC-SCs.

4. CONCLUSIONS

Aqueous $MnFe_2O_4$ CNC–SCs exhibit higher electrochemical performances than SC-HS due to the unique structure of CNCs. The effect of surfactants, namely SDS, Triton-X-100 and P123, added into $LiNO_3$ electrolyte is investigated based on the electrochemical characterizations of CNC-SCs. It is found that the presence of surfactants can significantly improve capacitance and decrease the surface tension of the electrode interface for better permeation of Li^+ ions. Upon the addition of SDS, the capacitance improves about 36.8% compared to the pure $LiNO_3$ electrolyte at 0.05 A/g. The capacitive

retention is about 82% after 1000 cycles, and the energy density is 14.5 Wh/Kg at 0.05 A/g. Triton-X-100 and P123 also exhibited positive effect on capacitance and capacitive retention, but to a less extent compared with SDS. The spacial configuration of surfactant is suggested to play an important role in determining the electrochemical properties of supercapacitors.

ACKNOWLEDGEMENTS
This work was financially supported the National Key Project on Basic Research (Grant No 2012CB722705), the National High Technology Research and Development Program of China (2012AA110407), the National Natural Science Foundation of China (No.s 21143006 and U1232104), the Foundation of Qingdao Municipal Science and Technology Commission (11-2-4-2-(8)-jch), and the Foundation of "Taishan Scholar" program of Shandong Province, China .

References

1. T. Y. Wei, C. H. Chen, H. C. Chen, S. Y. Lu and C. C. Hu, *Adv. Mater*. 22 (2010) 347.
2. P. Simon and Y. Gogotsi, *Nat. Mater*. 7 (2008) 845.
3. C. Liu, F. Li, L. P. Ma and H. M. Cheng, *Adv. Mater*. 22 (2010) E28.
4. M. Jayalakshmi and K. Balasubramanian. *Int. J. Electrochem. Soc.* 3 (2008) 1196.
5. S. L. Kuo and N. L. Wu, *Electrochem. Solid-State Lett*. 8 (2005) A495.
6. S. Trasatti and G. Buzzanca, *J. Electroanal. Chem*. 29 (1971) 1.
7. J. P. Zhang, P. J. Cygan and T. R. Jow, *J. Electrochem. Soc.* 142 (1995) 2699.
8. J. Xu, L. Gao, J. Cao, W. Wang and Z. Chen, *Electrochim. Acta* 56 (2010) 732.
9. Q. Lu, Z. J. Mellinger, W. G. Wang, W. F. Li, Y. P. Chen and J. G. Chen, *ChemSumChem* 3 (2010) 1367.
10. C. C. Hu and T. W. Tsou, *J. Power Sources* 115 (2003) 179.
11. Y. G. Wang and Y. Y. Xia, *Electrochem. Commun*. 7 (2005) 1138.
12. J. Y. Luo, W. J. Cui, P. He and Y. Y. Xia, *Nat. Chem*. 2 (2010) 760.
13. K. Fic, G. Lota, M Meller and E Frackowiak. *Energy Environ. Sci*. 5 (2012) 5842.
14. L. L. Zhang, T. Wei, W. Wang and X. S. Zhao, *Mater. Chem. Phys*. 116 (2009) 532.
15. F. Pico, E. Morales, J. A. Fernandez, T. A. Centeno, J. Ibänez, R. M. Rojas, J. M. Amar-illa and J. M. Rojo, *Electrochim. Acta* 54 (2009) 2239.
16. A. S. Adekunle, K. I. Ozoemena, B. B. Mamba, B. O. Agboola and O. S. Oluwatobi. *Int. J. Electrochem. Soc.* 6 (2011) 4760.
17. Z. J. Fan, J. Yan, T. Wei, L. J. Zhi , G. Q. Ning, T. Y. Li and F. Wei, *Adv. Funct. Mater*. 21 (2011) 2366.
18. K. Fic, G. Lota and E. Frackowiak, *Electrochim. Acta* 55 (2010) 7484.
19. J. Y. Ying, C. P. Mehnert and M. S. Wong, *Angew. Chem. Int. Ed*. 38 (1999) 56.
20. E. D. Goddard, K. P. Ananthapadmanabhan (Eds.), *Interactions of Sur-factants with Polymers and Proteins*, CRC Press, Florida (1993).
21. M. J. Rosen, *Surfactants and Interfacial Phenomena, 3rd ed.*, John Wiley & Sons, Inc., New Jersey (2004).
22. J. Kim, B. Kim, J. G. Lee, J. Cho and B. Park, *J. Power Sources* 139 (2005) 289.
23. H. X. Yang, Y. L. Cao, X. P. Ai and L. F. Xiao, *J. Power Sources* 128 (2004) 97.
24. N. L. Wu, S. Y. Wang, C. Y. Han, D. S. Wu and L. R. Shiue, *J. Power Sources* 113 (2003) 173.
25. P. Z. Guo, G. L. Zhang, J. Q.Yu, H. L. Li and X. S. Zhao, *Colloids and Surf.* A 395 (2012) 168.
26. L. Q. mai, F. Yang, Y. L. Zhao, X. Xu, L. Xu and Y. Z. Luo, *Nat. commun*. 2 (2011), 381(1–5).
27. S. L. Kuo and N. L. Wu, *Electrochem. Solid-State Lett*. 7 (2007) A171.

28. R. J. Robson and E. A. Dennis, *J. Phys. Chem*. 81 (1977) 1075.
29. D. Löf, A. Niemiec, K. Schillén, W. Loh and G. Olofsson, *J. Phys. Chem*. B 111 (2007) 5911.
30. V. Ganesh, S. Pitchumani and V. Lakshminarayanan, *J. Power Sources* 158 (2006) 1523.
31. Y. Liu, X. H. Qu, H. W. Guo, H. J. Chen, B. F. Liu and S. J. Dong, *Biosens. Bioelectron*. 21 (2006) 2195.
32. A. J. Bard, L. R. Faulkner, *Electrochemical Methods: Fundamentals and Applications, second ed.* Wiley, New York (2001).
33. T. Lu, Y. P. Zhang, H. B. Li, L. K. Pan, Y. L. Li and Z. Sun, *Electrochim. Acta* 55 (2010) 4170.
34. X. Li, J. P. Rong and B. Q. Wei, *ACS Nano* 4 (2010) 6039.
35. Y. P. Lin and N. L. Wu, *J. Power Sources* 196 (2011) 851.
36. S. L Kuo, J. F. Lee and N. L. Wu, *J. Electrochem. Soc*. 154 (2007) A34.
37. R. B. Rakhi, W. Chen, D. Cha and H. N. Alshareef, *Adv. Energy Mater*. 2 (2012) 381.

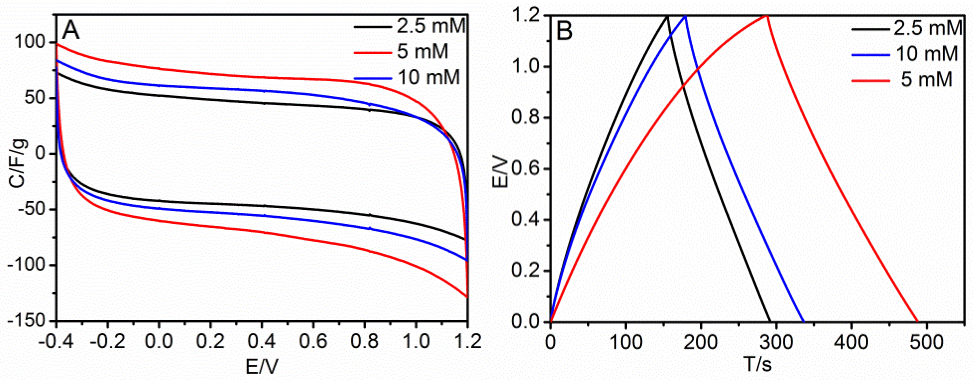

ESI Figure 1. CV (A) and galvanostatic charge–discharge (B) curves of CNC-based supercapacitors with the addition of SDS under different concentrations. Scan rate in ESI Figure 1A: 20 mV/s.